ELSEVIER

Journal of Nuclear Materials 289 (2001) 308–314

journal of nuclear materials

www.elsevier.nl/locate/jnucmat

# Absorption of molten fluoride salts in glassy carbon, pyrographite and Hastelloy B

J. Vacik [a,b,*], H. Naramoto [a], J. Cervena [b], V. Hnatowicz [b], I. Peka [c], D. Fink [d]

[a] *Advanced Science Research Center, Japan Atomic Energy Research Institute, Watanuki 1233, Takasaki, Gunma 370-1292, Japan*
[b] *Nuclear Physics Institute, Academy of Sciences of Czech Republic, CZ 250 68 Rez, Czech Republic*
[c] *Nuclear Research Institute plc, CZ 250 68 Rez near Prague, Czech Republic*
[d] *Hahn-Meitner-Institute, Glienicker Str. 100, D-14109 Berlin, Germany*

Received 9 September 2000; accepted 12 December 2000

**Abstract**

Materials performance is one of the issues of the accelerator driven transmutation technology (ADTT). Identification of the materials, which would satisfy the strength and integrity requirements for the target–blanket assembly (e.g. corrosion and radiation resistance), is a significant challenge. We report on the study of the interaction (i.e. penetration and capture) of molten fluoride salts with glassy carbon, pyrolitic graphite, and Hastelloy B, which are considered as candidates for structural materials of the ADTT systems. Massive penetration into and capture of molten fluorides within a several micrometer thick surface layer was observed for all inspected specimens. The incorporation rate of the molten fluorides depends on the exposure time and temperature of the molten fluoride bath. The corrosion resistance of the specimens was verified in stationary conditions. Whereas excellent resistance has been found for pyrolitic graphite, evident corrosion was observed for glassy carbon and particularly for Hastelloy B. 

*PACS:* 28.41.Kw; 28.41.Qb; 29.20.Mr; 29.30.Ep

## 1. Introduction

The use of the 'particle accelerator – neutron multiplying assembly' concept for commercial nuclear energy production without a long-term high-level waste stream and transmutation of both fission products and higher actinides has been under consideration for many years [1,2]. Recently, the concept of the hybrid reactor has been renewed, in particular, due to a growing awareness of the nuclear wastes of spent nuclear fuel, weapon grade plutonium and highly enriched uranium from naval reactors [3–5]. Several different hybrid systems for neutron-induced transmutation of long-living radioactive nuclei of the nuclear waste have been designed, however no one has been generally accepted up to now (see the discussion in e.g. Refs. [6–8]). The current view of the accelerator driven transmutation technology (ADTT) is based on the experience obtained during the molten salt reactor experiment (MSRE) in Oak Ridge National Laboratory (ORNL), USA [9] and experiments carried out in several other countries (see papers in [6–8,10]).

The ADTT assembly includes, in principle, a powerful proton accelerator (typically 10 mA of 1 GeV protons) feeding an intensive neutron spallation source (e.g. liquid Pb or eutectic Pb + Bi), a subcritical vessel surrounding the spallation target, and a system for separation of fission and transmutation products. Molten fluoride (MF) salts or molten metals (e.g. Pb) serve as a coolant of the reactor part and as a carrier of nuclear fuel (several wt%) dissolved in the media. The nuclear waste is incinerated and transmuted by neutron irradiation in the accelerator-driven blanket towards

* Corresponding author. Tel.: +81-27 346 9429; fax: +81-27 346 9699.
*E-mail address:* vacik@taka.jaeri.go.jp (J. Vacik).

0022-3115/01/$ - see front matter 
PII: S0022-3115(01)00419-6

stable nuclei or short-living species, which are on-line separated, and then kept in the storage until they decay to an admissible level.

ADTT concepts offer obvious advantages (as compared to the classical critical reactors), which are, however, counter-balanced by their great complexity. Apparently, ADTT projects require extensive investigation of numerous questions. Such issues as a powerful accelerator capable of driving a target–blanket assembly, an effective neutron spallation source, optimal chemistry of the fluid–fuel system, fast and continuous fission product separation, etc. are under intensive discussion and laboratory tests. Corrosion of the ADTT structural components is one of the serious problems requiring attention. Very high radiation load and chemical aggressiveness of the hot working media in the hybrid reactor may seriously complicate the proposed schema. In the designed ADTT systems, high-level resistance to radiation damage by neutrons and charged particles and high-level resistance to corrosion by molten salts or metals are basic criteria, which must be satisfied.

Generally, the damaging effects of neutrons and energetic particles on materials arise from knocking atoms out of their lattice sites and/or from accumulation of the gaseous transmutation products (i.e. He, T and H). Atomic displacement by neutron elastic scattering is possible only above neutron energy of about 400 eV for materials with the atomic mass around 50. Gas production can arise from neutron induced charged particle reactions (with threshold around 5 MeV) on some nuclei. Both effects may lead to extensive microstructural alterations (such as void swelling, irradiation creep, radiation-induced stress and cracking, etc.) that might have important macroscopic consequences (e.g. material deformation, embrittlement, etc.). As a result of an intensive neutron and energetic particle irradiation, irreversible changes in mechanical properties are induced, which can become an inadvertent life-limiting factor for the structural components of the ADTT systems.

Corrosion of the materials depends on the composition and working temperature of the solvent media. It can have a substantial effect on the redox chemistry of the whole system and deeply affect corrosion rates. In principle, the solvent media have to exhibit high solubility of the actinides and fission products, sufficient radiation stability and suitable thermodynamic and physical properties such as relatively low melting point, good viscosity, thermal stability, heat content and low vapor pressure. The medium in the form of a MF salt, which enables easy manipulation using the fluoride volatility process, has a working temperature well above 500°C. The LiF salt can be molten at high temperatures around 995°C (isotopically pure isotope $^{7}$Li is needed as a constituent of the LiF compound to prevent gas production via intensive nuclear reaction $^{6}Li(n_{th}, \alpha)T$ on the 7.59% naturally abundant isotope $^{6}$Li). To achieve a lower melting point (and consequently a lower corrosion effect), two or more salts should be combined; e.g. the fluoride solvent $LiF + BeF_2$ (2:1 mole ratio) used in MSRE has a melting point of 425°C [9].

Nickel based alloys (e.g. Hastelloy N, which seemed to be satisfactory in ORNL conditions) are primarily considered as construction materials for ADTT reactor vessels. It has been demonstrated that the fluoride salts can be stored in the nickel alloys with very low corrosion rates (though an aggressive attack on the container has been observed during molten fluoride salt processing) [9]. Nickel in the alloy, however, can suffer high damaging rates from neutron induced gas production (via the nuclear reactions (n, $\alpha$) and (n, p) on the 68% naturally abundant isotope $^{58}$Ni). The target–blanket assembly should therefore be shielded by a suitable material (e.g. carbon based cover), which would serve as a neutron reflector and also protect the vessel against the aggressive solvent medium.

The issue of corrosion resistance of construction materials considered for the ADTT systems has become a matter of frequent investigation [6–8]. A variety of mixtures of the MF salts as basic matrixes of the nuclear fuel and cooling circuits are currently discussed and the effect on selected materials is analyzed. One of the particular problems bearing on the corrosion–erosion process, which has not yet been well examined, is the penetration/absorption of the MF salts in the materials enhanced by the elevated temperature of the solvent bath. Basically, the penetration of the fluoride species into materials can proceed in different ways depending on the microstructure of the specimens, e.g. in non-porous materials penetration will be restrained while accelerated for porous structures. The influence of the molten fluorides (absorbed in the materials) on the corrosion process is not clear. Nevertheless, massive absorption of the MF salts in the presence of intensive neutron irradiation might induce microstructural alterations, which can degrade the materials and weaken the mechanical integrity of the system. In our previous study [11] several carbon allotropes and metal specimens were examined and preliminary results of rapid penetration and capture of the MF salts in the samples were reported. In the present study, a more detailed inspection of the selected specimens, i.e. glassy carbon, pyrolitic graphite and nickel-based Hastelloy B, has been performed and more complete results are presented.

## 2. Experimental

Various nuclear techniques are available for the analysis of composition and structure of surface layers of solids. These techniques, using ion or neutron probing beams, can determine concentration depth profiles of

practically all elements in materials up to the depth of several micrometers. Generally, these techniques exhibit high sensitivity and excellent depth resolution and are suitable for the non-destructive study of the diffusion and corrosion processes prompted in ADTT related materials by fluoride media [11].

In this work, thermal neutron depth profiling (NDP) [12,13] has been utilized for the analysis of Li (component of LiF) absorbed in the examined specimens. The NDP technique is based on the (n, α) or (n, p) exoenergetic nuclear reactions induced by thermal neutrons on several light elements (e.g. He, Li, B, N, Cl). When analyzed, the samples are irradiated with a well-collimated neutron beam and the reaction products (protons, tritons, alpha particles) are registered with a suitable detector system placed in a certain distance from the target. The depth distributions of the elements can be reconstructed from the residual energy of the particles escaping from the samples. In standard experimental conditions, the typical detection limit for Li is about 1 at. ppm and the depth resolution is about 50 nm. Because of interference from other reaction products, the accessible depth region in the case of the carbon allotropes is about 7 μm and about 3 μm for the metallic specimens. The present experiment was carried out at the LWR-15 nuclear research reactor in Rez [14] on a thermal neutron beam (collimated by a short neutron guide) with an intensity $\sim 10^7$ $n_{th}$ $cm^{-2}$ $s^{-1}$ and Cd ratio $\sim 10^5$.

Several commercially available carbon allotropes (glassy carbon and pyrolitic graphite) and nickel-based Hastelloy B were selected for the experimental test. Each specimen was cleaned with ethyl alcohol and in boiling water (1 h) and after this divided into several pieces, each with an area of about 1 $cm^2$. The thickness of the samples was about 1 mm (Hastelloy B) or 2 mm (carbon allotropes). One unmodified (pristine) piece was kept for comparison. The purified samples were treated in a programmable resistance furnace in a bath of MF salts, either in one-component LiF (100%) with a temperature of 995°C or in a mixture of LiF (46.5 wt%) + KF (42 wt%) + NaF (11.5 wt%) (FLiNaK) with a melting point of 540°C. The samples were isothermally exposed either for 1 h to LiF (except of Hastelloy B) or for 1, 5 and 10 h to FLiNaK. After the exposure the specimens were leached in boiling distilled water for 1 h to remove free LiF molecules from the bulk and salt remnants from the surface (they could seriously interfere with the analysis), cleaned again in ethyl alcohol and compared by the following NDP measurements.

## 3. Results and discussion

Nickel based alloys, such as Inconel, Nickelvac or Hastelloy, are serious candidates for the structural materials of the molten salt loops in the subcritical reactor assembly. For the interaction/absorption test Hastelloy B (N10001) based on Ni (65%) and Mo (28%) (minor elements like Fe, Cr, C, Si, Ti, Co, Mn, Al and W balance the composition) was subjected. Typical energy spectra of Li captured in Hastelloy B before and after exposure to FLiNaK at temperature 540°C for 5 h are demonstrated in Fig. 1. The nuclear reaction $^6Li(n_{th}, \alpha)T$ ($\sigma = 940$ b, $Q = 4785$ keV) induced by thermal neutrons enabled us to analyze the Li depth distribution up to about 3.5 μm. For the depth profile evaluation only the energy spectrum between the alpha-particle and triton peaks was taken into account to avoid interference from the alpha-particle signal. The Li depth profiles are shown in Fig. 2 for untreated (pristine) and treated Hastelloy B specimens. Similarly to the previous experiment [11], the depth profiles give evidence of rapid and massive penetration of the MF salts to the sample. The

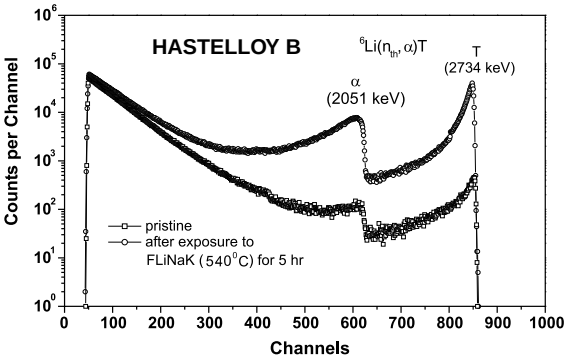


Fig. 1. Energy spectra from the reaction $^6Li(n_{th}, \alpha)T$ measured on Hastelloy B before and after exposure to the molten fluoride salts LiF + KF + NaF (FLiNaK) at temperature 540°C for 5 h. For evaluation of the Li depth profiles, only the region between triton and alpha peaks was taken into account.

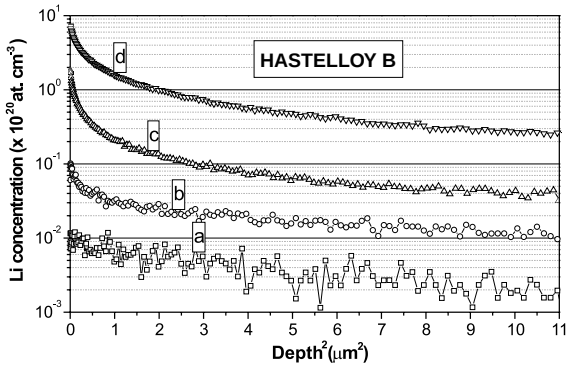


Fig. 2. The Li depth profiles measured by the NDP technique on Hastelloy B before (a) and after exposure to FLiNaK (540°C) for 1 h (b), 5 h (c) and 10 h (d).

content of Li near the surface in the pristine sample is about 100 ppm. The value decreases gradually with the depth and falls to about its half in 3 μm. When exposed to the MF salts, the concentration of Li in the surface region is growing significantly. After the 1-h exposure to FLiNaK, the Li concentration (i.e. LiF compound) has increased by about 5 times in the whole accessible range and by about 1 order of magnitude near the surface. The exposures for 5 and 10 h have enriched the Li content by about 1 or 2 orders of magnitude, especially in the first micrometer of the depth. The profiles have rather complicated non-uniform character. In their surface-far parts they are characterized by linear curves in the plots of concentration vs. depth$^2$. As the evolution of the profiles with exposure time corresponds roughly to the Fickian diffusion into a semi-infinite solid, one can estimate, from the linear part, the effective diffusion coefficient. The obtained value $D = 3 \times 10^{-13}$ cm$^2$ s$^{-1}$ is about 1.5 times lower than that previously measured on the nickel foils [11].

Glassy carbon (GC) is considered as a primary construction material for the neutron reflector and inner protector of the target – blanket assembly [15]. It can be prepared by slow, controlled degradation of certain polymers at high temperatures, typically on the order of 900–1000°C [16]. GC consists of randomly oriented graphite-like ribbons (about 100 Å long and 30 Å in cross-section) and has a porous but impermeable glass-like structure. Depending on the processing conditions the porosity can vary from near zero up to several tens of percent with the pores mean separation of about 1 nm [16]. Unlike graphite, GC has no long-range order in three dimensions, which makes it chemically more inert than graphite. In Fig. 3, the depth distributions of Li in pristine and treated specimens are shown. The shape of the profiles is similar as in Hastelloy B, i.e. with a dominant precipitation of Li near the surface region

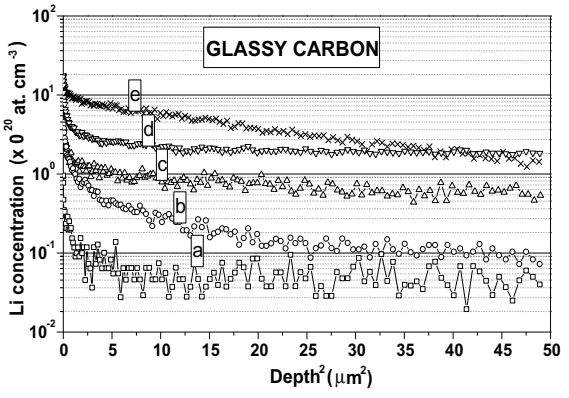


Fig. 3. The Li depth profiles in glassy carbon before (a) and after exposure to FLiNaK (540°C) for 1 h (b), 5 h (c), 10 h (d) and LiF (995°C) for 1 h (e).

(here with the thickness of about 1–2 μm) and constant slow decline towards the bulk. Surprisingly, pristine GC already contains about 500 ppm of Li near the surface, this value however rapidly decreases and in the 3 μm depth it is 1 order of magnitude lower. The first exposure to FLiNaK for 1 h has increased the content of Li in the first 2 μm by 1 order of magnitude – hence substantially, though in the depths above 4 μm this increase amounts to only about 2 times. It is evident that during the 1-h exposure Li penetrates rapidly through the pores near the surface, however cannot balance the content within the broad range. The 5-h exposure is a sufficient time for the massive incorporation of Li with an almost uniform concentration profile in the whole accessible range (except of the first micrometer). The concentration of Li (1 order of magnitude higher as compared with the pristine sample) declines only slightly with the depth (with a small linear regression slope $b = -0.0055$). A similar pattern can also be seen for the 10 h exposure, however, with a higher (15 times above the pristine value) and more uniform ($b = -0.0027$) concentration level. The penetration of the MF salts to GC with a porous structure is a complex transportation process. The MF salts enter the sample not only through the system of pores (e.g. by percolation process) but also through the non-porous parts (i.e. by Fickian diffusion process). These two processes compete with each other. Because the porosity of GC can vary in different samples [16], one of the two above-mentioned mechanisms might prevail. It is evident that the form and the evolution of the Li depth profiles in Fig. 3 do not resemble the random walk diffusion patterns, which would demand uniform shapes and corresponding concentrations. One can therefore attribute the measured Li depth profiles to percolation rather than to diffusion mechanism. Nevertheless, to estimate the 'penetration rate' of MF salt to GC the 'effective diffusion coefficient' can be deduced from the profiles. The estimated value $D \sim 1.5 \times 10^{-12}$ cm$^{-2}$ s$^{-1}$ is about 1 order of magnitude higher than that for Hastelloy B (see above). When GC is exposed to molten LiF at temperature of 995°C the penetration of the fluorides is most forceful. After exposure the content of Li has increased by about 2 orders of magnitude above the pristine level. The depth profile indicates that the MF salts penetrates deeply into the bulk, but similarly as to the 1-h exposure to FLiNaK (540°C) the exposure time is not sufficient for Li to balance the concentration in the whole inspected depth. The profile can be described as a result of fast percolation with the 'effective diffusion coefficient' $D = 3 \times 10^{-11}$ cm$^{-2}$ s$^{-1}$.

Another carbon allotrope considered as structural material for inner shielding of target–blanket assembly is pyrolitic graphite [15]. Pyrographite is a specific form of elemental carbon produced from hydrocarbons in gaseous phase at temperatures above 2000°C. It consists of

parallel $c$-basal planes with large single crystal graphite flakes and exhibits properties close to those of single crystalline graphite, however with a high degree of $c$-axis alignment. Pyrographite was treated in the MF salts in the same way as GC. The resulting Li depth profiles for the pristine and treated samples are shown in Fig. 4. As can be seen, the depth profiles are complicated in the form and irregular in the evolution. The content of Li in the pristine sample is about 10 ppm near the surface. This value slowly decreases with the depth to the 5-ppm level. The 1-h exposure to FLiNaK (540°C) has elevated the content of Li by about 5 times, exposure for 5 h by about 20 times. Similarly to GC, the profiles in the {concentration vs. depth$^2$} plot consist of a dominant outer part (~2 μm) and a straight inner region. From the linear part of these two profiles the effective diffusion coefficient can be extracted. The value $D = 2 \times 10^{-14}$ cm$^{-2}$ s$^{-1}$ is the lowest one from the aforesaid data. Exposure for 10 h has increased the content of Li only in the first 5 μm by about 5 times, and at the same time the profile in the deep region 6–7 μm has almost not changed. Surprisingly, in contrast to the other profiles, at the surface no dominant absorption has been observed. Instead, a rather broad region (~2 μm) with an almost constant Li content has been formed. A similarly broad region can also be seen in the Li distribution after exposure to LiF (995°C) for 1 h, which has elevated the Li content by about 2 orders of magnitude above the pristine level. In this case, however, the region spans the inner broad part from 2 to 7 μm, whereas near the surface the Li concentration is almost 10 times higher. The reason for this behavior is not clear, however one should take into account the flake-layered structure of the pyrographite and its possible influence on the mobility of the dopants.

Fig. 5 compares Li concentration of Hastelloy B, GC and pyrographite in the first 3 μm thick region before and after exposure to the MF salts. All specimens exhibit an initial rapid growth in the Li content after the first hour of exposure to FLiNaK. The increase is however not uniform; the lowest is for pyrographite, the highest for GC. The incorporation rate (in at. Li/h) between 1 and 10 h exposure to FLiNaK can be estimated as follows: $3.5 \times 10^{19}$ for GC, $1.7 \times 10^{18}$ for Hastelloy B and $9.5 \times 10^{17}$ for pyrographite. In the case of Hastelloy B, the incorporation rate is close to the value observed in the experiment with the nickel foil [11]. The reason for Li absorption might be the existence of a thin oxidized surface layer, into which the MF salts can diffuse and precipitate. A big difference in the incorporation rate between GC and pyrographite documents the dissimilarity in the structure of both carbon allotropes. The enhanced absorption of the MF salts in GC can evidently be attributed to its porous structure; the MF salts more easily penetrate in molar quantity to the open pores and can be entrapped there. In pyrolitic graphite with close basal planes and large graphite flakes the incorporation of the MF salts is more restricted.

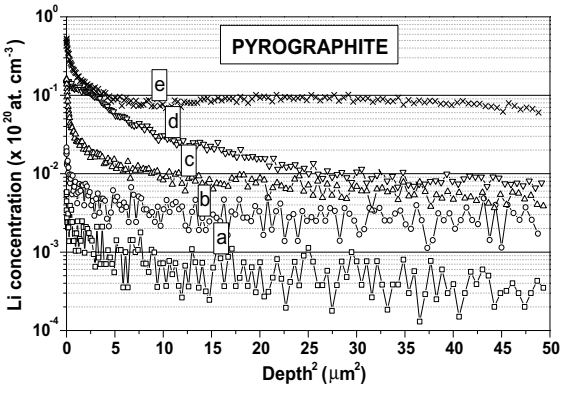


Fig. 4. The Li depth profiles in pyrographite before (a) and after exposure to FLiNaK (540°C) for 1 h (b), 5 h (c), 10 h (d) and LiF (995°C) for 1 h (e).

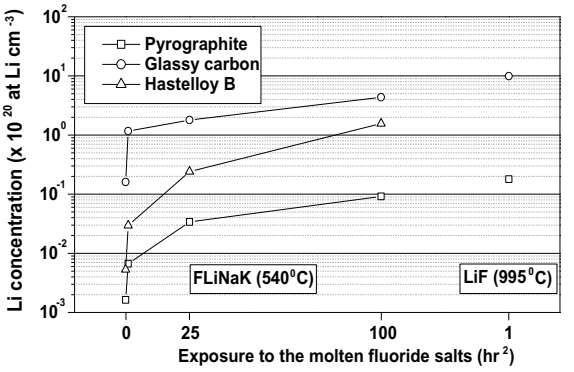


Fig. 5. Comparison of the Li content in the first 3 μm thick layer in Hastelloy B, glassy carbon and pyrographite, as plotted via the square of time.

The corrosion resistance of the inspected specimens was surveyed by measuring of weight loss of the samples after each treatment in the MF salts. Table 1 documents the relative change in the weight of the specimens (the weight gain due to the absorption of the MF salts is $<10^{-6}$ wt% in the present conditions and does not affect the measurement). In case of pyrographite, no difference (with a precision of $10^{-4}$) in the sample weight before and after exposure has been registered. Pyrographite remained chemically intact during the first hours of exposure to LiF or FLiNaK, though about $10^{-4}$ at.% Li has been absorbed in the surface region. For GC, however, about 0.5% weight loss has been observed. The reason is not clear. It might be a consequence of the massive incorporation of the hot MF salts (1 or 2 orders of magnitude higher than for Hastelloy B or pyrographite, respectively) which, in principle, can affect the mechani-

Table 1
Weight loss (in %) of specimens after exposure to the molten fluoride salts

| Specimens | LiF 995°C, 1 h | LiF + KF + NaF 540°C, 1 h | LiF + KF + NaF 540°C, 5 h | LiF + KF + NaF 540°C, 10 h |
|---|---|---|---|---|
| Hastelloy B | 1.4 | 0.5 | 1.2 | 2 |
| Glassy carbon | 0 | 0 | 0.5 | 0.5 |
| Pyrographite | 0 | 0 | 0 | 0 |

cal strength of the porous material by inducing a substantial stress in the surface region. Another possible corrosion mechanism is discussed below. Depending on the processing, GC can be treated in a manner, which reduces their porosity to a near-zero level. Thus by lowering the availability of the pores, the absorption of MF salts in GC can be restricted. The most pronounced corrosion was observed for Hastelloy B. After the 10 h exposure to LiNaK about 2% of its weight was lost. The reason is not clear. It should be noted that there is no reason for any chemical interaction of the MF salts with nickel (and other constituents of Hastelloy B), as well as with carbon (GC, pyrographite). The corrosion effect, which has nevertheless been observed, might perhaps be explained by the presence of the reactive trap constituents (such as oxygen or nitrogen) in the MF solvent or even in the inspected specimens (oxygen is known to remain in GC even though heat-treated at high temperatures). At the temperatures of the MF salt exposures, such constituents would react rapidly with the specimens to form the products, which would be easily dissolved in the salt melt (e.g. in the case of carbon, the likely product would be gaseous CO or $CO_2$).

Though the corrosion resistance of pyrographite was found to be excellent and relatively good for GC, it should be noted, that under intense neutron bombardment the degradation of pyrographite (as well as GC and Hastelloy B) might be prompted due to the radiation induced destructive processes. One of the mechanisms of microstructural alterations is above-mentioned embrittlement due to the neutron induced gas production. In fact, helium, tritium and hydrogen gas can originate in neutron induced transmutation of e.g. Ni (Hastelloy B) and/or Li (LiF absorbed in materials) in the $^{58}Ni(n, p)^{58}Co$, $^{58}Ni(n,\alpha)^{55}Fe$, $^{7}Li(n,\alpha,n)^{3}H$ and two-step $^{7}Li(\gamma, n)\ ^{6}Li \rightarrow {}^{6}Li(n_{th}, T)^{4}He$ nuclear reactions. Another mechanism of material degradation can be radiation knock-out damage, which, at higher neutron fluences, can lead to a rapid loss of mechanical properties, e.g. for graphite at the fluence above $10^{22}$ n cm$^{-2}$ s$^{-1}$ (ADTT systems are supposed to operate with high neutron fields around $10^{16}$ n cm$^{-2}$ s$^{-1}$). On the other hand, the elevated temperatures enable an efficient material re-crystallization and defect annealing, as well as fast gas removal, due to the material components self-diffusion and considerable mobility of the formed gas bubbles.

## 4. Conclusion

The exposure of GC, pyrolitic graphite and Hastelloy B to the molten fluoride salts (LiF or LiF + NaF + KF) results in rapid penetration of the molten fluorides to the inspected specimens. The molten fluorides are absorbed in large quantities (in case of GC up to several at.%) in the first micrometers of the depth with dominant precipitation at the surface. The MF salts incorporation rate is dramatically enhanced by the temperature of the fluoride bath.

Corrosion resistance, verified in stationary, conditions was found distinctive for pyrolitic graphite, which remained chemically intact. Evident corrosion effect was, however, observed for GC and particularly for Hastelloy B. The corrosion mechanism of GC and Hastelloy B is not clear. It might bear on the possible presence of the reactive impurities (such as oxygen and nitrogen) in the fluoride salt bath and/or in the specimens' structure, which would rapidly react at the temperatures of exposure with the materials.

The aim of this study was to investigate the reactivity (in the sense of penetration and absorption) of the selected materials with the molten fluoride salts. The results clearly demonstrate, that GC, pyrographite and Hastelloy B, the possible candidates for the construction materials of the ADTT reactors, can absorb molar quantity of molten fluorides even though exposed to the solvent media only for several hours. This, in principle, might enhance the degradation of the materials in real conditions of the ADTT systems where intense gamma, ion and neutron fields would exist.

## Acknowledgements

The work was supported by Grant Agency of the Czech Republic under the projects No. 202-96-0077 and 202-97-K038. One of the authors (J.V.) would like to express his thanks for support of the work also by Japan

Atomic Energy Research Institute under the program of JAERI Research Fellowship.

## References

[1] W.B. Lewis, Report of Atomic Energy of Canada Limited AECL-968, 1952.
[2] L.C. Hebel, E.L. Christensen, F.A. Donath, W.E. Falconer, L.J. Lidofsky, E.J. Monoz, T.H. Moss, R.L. Pigford, T.H. Pigford, G.I. Rochlin, R.H. Silsbee, M.E. Wrenn, Rev. Mod. Phys. 50 (1978) Part II, p. 1.
[3] C. Rubbia, J.A. Rubio, S. Buono, F. Carminati, N. Fietier, J. Galvez, C. Geles, Y. Kadi, R. Klapisch, P. Mandrillon, J.P. Revol, Ch. Roche, Conceptual Design of a Fast Neutron Operated High Power Energy Amplifier, CERN/AT/95-44 (ET), September 29, 1995. See also [4].
[4] C. Rubbia, in: AIP Conference Proceedings 346, International Conference on Accelerator-Driven Transmutation Technologies and Applications, Las Vegas, NV, July 25–29, 1994.
[5] C.D. Bowman, E.D. Arthur, P.D. Lisowski, G.P. Lawrence, R.J. Jensen, J.L. Anderson, B. Blind, M. Cappiello, J.W. Davidson, T.R. England, L.N. Engel, R.C. Haight, H.G. Hughes III, J.R. Ireland, R.A. Krakowski, R.J. LaBauve, B.C. Letellier, R.T. Perry, G.J. Russell, K.P. Staudhammer, G. Versamis, W.B. Wilson, Nucl. Instrum. and Meth. A 320 (1992) 336.
[6] Proceedings of the First International Conference on Accelerator Driven Transmutation Technologies and Applications, Las Vegas, NV, July 25–29, 1994.
[7] Proceedings of the Second International Conference on Accelerator-Driven Transmutation Technologies and Applications, Kalmar, Sweden, June 3–7, 1996.
[8] Proceedings of the Third International Conference on Accelerator-Driven Transmutation Technologies and Applications, Prague, Czech Republic, June 7–11, 1999.
[9] A.M. Weinberg, Nucl. Appl. Technol. 8 (1970) 102.
[10] V.M. Novikov, V.V. Ignatiev, V.I. Fedulov, V.N. Tcherednikov, Liquid Salt Nuclear Reactors, Energoatomizdat, Moscow, 1990.
[11] J. Vacik, V. Hnatowicz, J. Cervena, V. Perina, R. Mach, I. Peka, Nucl. Instrum. and Meth. B 139 (1998) 264.
[12] R.G. Downing, G.P. Lamaze, J.K. Langland, J. Res. Nat. Inst. Stand. Technol. 98 (1993) 109. See also [13].
[13] D. Fink, Report of Hahn-Meitner-Institute, HMI-B 539, 1996.
[14] J. Vacik, J. Cervena, V. Hnatowicz, V. Havranek, D. Fink, Acta Physica Hungarica 75 (1994) 369.
[15] V.M. Novikov, V.V. Ignatiev, V.I. Fedulov, V.N. Tcherednikov, Liquid Salt Nuclear Reactors, Energoatomizdat, Moscow, 1990.
[16] G.M. Jenkins, K. Kawamura, Polymeric Carbons – Carbon Fiber, Glass and Char, Cambridge University, Cambridge, 1976.